MAFSA

Mars Autonomous and Foldable Solar Array

University of Colorado, Boulder

Nick Glascock[1], Bryce Huber[2], Eric Robinson[3], Will Evonosky[2], Clayton Cantrall[2] and Project Advisor Kyri Baker[4]

[1]*Department of Electrical Engineering,* [2]*Department of Aerospace Engineering,* [3]*Department of Mechanical Engineering,* [4]*Department of Civil, Environmental, and Architectural Engineering*

Contents

1 Introduction

As NASA looks towards Mars for the next frontier of human space exploration, there is a need to prepare supporting technologies that will allow humans to live on the red planet for an extended duration. We have designed a low-mass, autonomously deployable solar array that will generate the required power for scientific, habitat, and in-situ resource utilization functions necessary for a human mission to Mars.

The system was designed with three main driving requirements in mind: The stowed volume must be no greater than 10 m^3, the mass must not exceed 1500 kg, and the total photovoltaic charging area must be a minimum of 1000 m^2. The volume requirement, coupled with an assumed cylindrical lander profile, meant that increases to lander radius constrained the height profile of the solar arrays and vice versa. It was decided that a lander radius of 2.5 m and, therefore, an allowed stowed height of 0.5 m would best fit the needs of our system.

The design uses five flexible booms that are stowed in a wrapped configuration around a central hub. The stowed height of the booms is 20 cm, allowing for an additional 30 cm of height used for stowing the folded solar array around an upper hub. During deployment, two electric motors will rotate the hubs, forcing the booms to extend out of the lander and the solar array to unfold into a pentagon pattern. The array can also be retracted with the ability to resume its original stowed configuration for dust and storm mitigation.

In the deployed state, the area of the array will be slightly greater than 1000 m^2, with 21 m booms extending to the corners of the pentagon. Each fifth of the pentagon array is designed with 80 radial fold lines that allow for a stowed height of 30 cm. Dust mitigation is accomplished by partially retracting the booms, and allowing dust to fall through holes placed in the troughs of the array. During partial retraction, the array transitions from a flattened surface to a zig-zag along the fold lines, allowing for 80 sections in each module to be angled towards the ground.

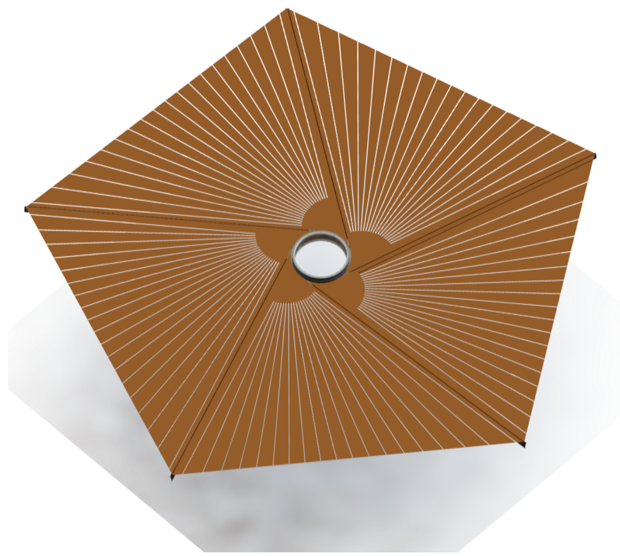

Figure 1: Fully deployed array

The following sections address the motivation for MAFSA, the technologies and their integration which comprise the foundation of the array design, and finally, the mission plan for the array to successfully operate for 10 years on a dynamic Martian surface.

2 Motivation for MAFSA

In developing MAFSA, several concepts were investigated and later discarded due to their inability to meet the design requirements set forth by NASA. One aspect of many early concepts that repeatedly drove the system out of specification was rigid booms. We investigated telescoping, folding, and combinations of the two types of booms, but they always drove the system above the mass or volume requirement. From this early experience, it was decided that any future concept utilizing some variation of a boom should incorporate materials or technologies that were flexible for storage yet rigid enough to support a large solar array.

After several concept failures, two were deemed worthy of in-depth consideration. One of the concepts was MAFSA as described in this paper, the other utilized an inflatable ring structure. The inflatable would fill with air pumped from the Martian atmosphere and subsequently push itself into a large ring around the original lander. This ring would have pulleys and cables connected to the middle lander which would pull the solar array into place with a motor. This design was excluded for three main reasons:

1. The ring structure would be required to drag across the Martian surface as it inflated causing risk of puncture and or snagging on large objects.

2. The ring would require constant re-inflation due to natural pressure loss leading to constant on-off cycling of the pumps.

3. Fabrication of inflatable materials has been a challenge since inflatables were first proposed for space applications.

This leads to MAFSA as currently presented. MAFSA includes both new technologies and new applications of existing technologies that conform to the design constraints set forth by NASA.

3 Existing Technologies

3.1 Deployable Boom

The flexible booms used in this design are a scaled up version of Triangular Rollable and Collapsible (TRAC) booms originally invented by the Air Force Research Laboratory and developed by Roccor. When stowed, the booms take on a flattened shape minimizing stowage volume, and allowing them to wrap 360°. When deployed, the booms unfurl at one end to allow for maximum axial and vertical strength. Up to this point TRAC booms have only been used in CubeSat applications where the maximum boom length was 4 m. [1] The booms are made from unidirectional Hexcel® IM7/977-2 carbon fiber composite.

3.2 Retraction and Deployment Motor

Two 3-phase, 4-pole induction electric motors will be used for rotational deployment and retraction of the booms. An example of this motor can be found in a Tesla Roadster and is capable of producing up to 185 kW of power output with a maximum torque of 270 Nm.

3.3 Bearings

Kaydon NG series bearings will be used for rotation of the booms and array about the central shaft. NG series bearings are a lightweight ball-bearing designed for radial loads. Kaydon manufactures these bearings up to a 1 meter outside diameter. To meet the specifications of MAFSA, the bearings will need to be scaled to an outside diameter of 4 m. The estimated mass of the scaled bearing is approximately 54 kg. The estimated thickness of the bearing is 5 cm. The bearing is capable of operating up to a approximately 300 kN radial load and up to a 750 kN thrust load [2].

3.4 Photovoltaics

XTJ Prime triple junction thin film solar cells from Spectrolab will be used for the solar array. These cells were chosen over solar cells from Alta Devices, SolAero, and Azur Space for their low relative mass and comparable efficiency. Spectrolab solar cells come in a 3.97 cm by 6.91 cm rectangular cell size. The area mass density is 500 g/m^2. These cells have a beginning of life efficiency of 30.7% and an end of life efficiency of 26.7%. The thickness of the cells ranges from 60-225 μm [3].

3.5 Solar Cell Substrate

DuPont Kapton PV9100 Series polymide film will be used as the solar cell substrate. The material has been successfully implemented in space PV applications, and provides protection to the thin film cells. It has a thickness of 50μm [4].

4 Design Overview

MAFSA can be broken down into 3 primary components: the central hub, the booms, and the solar array. Each component will be discussed individually followed by a description of the mechanical relation between each component. Finally, a short description of the lander design for MAFSA will be discussed.

4.1 Central Hub

The hub is composed of two stacked central aluminum cylinders with a fixed metal plate separating both cylinders (mid plate), and a fixed base metal plate upon which MAFSA is constructed. A central shaft, 3.9 m in diameter, runs from the base plate to the top of the module. Above the base plate is the 20 cm tall, 4.9 m diameter cylinder used for boom stowage. The base plate and mid plate are joined by 16, 20 cm tall, aluminum supports that are positioned at the outer perimeter of the plates. The upper cylinder is 30 cm tall and 4 m in diameter for array stowage. Each cylinder is mounted to the fixed central shaft using a bearing system that allows for rotational motion. The two sections are constructed so that the lower section provides boom compactness, discussed below, and the upper section allows the array to deploy without obstruction.

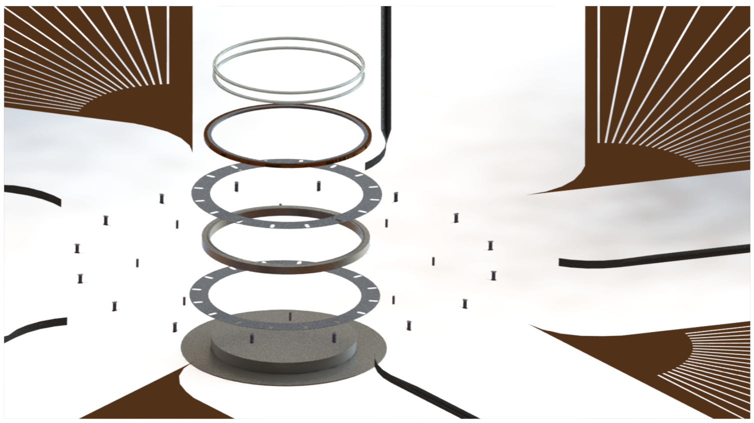

Figure 2: Exploded view of hub

In addition to the supports attaching the upper and lower plates, 16 spring-fixed rollers, as shown in Figure 3, will be lined along the outside of the lower cylinder section. These rollers will guide boom wrapping as tightly as possible, preventing severe buckling in the boom.

To assist with deployment, there will be 5 additional guiding rollers located at the points where booms will be transitioning from a stowed state to a deployed state. These rollers will set boundary conditions as the booms unfurl at their open ends, and will assist in a straight-line deployment tangent to the hub. Additionally, a brush will be placed outside of the guiding rollers to sweep dust from inside the booms upon retraction.

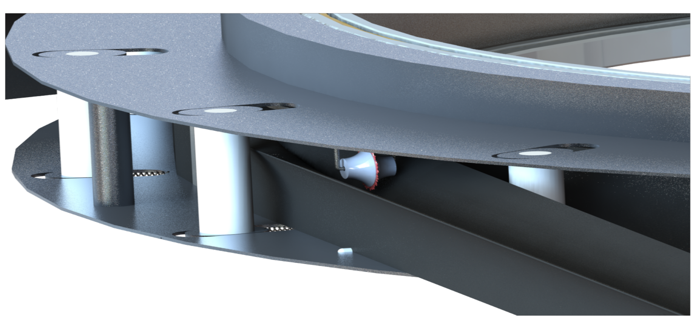

Figure 3: Rollers allowing booms to transition from stowed to deployed state

The battery and power electronics will be stowed inside of the lower aluminum cylinder. These components will lie on the lower plate of the hub while being protected from outside influences by the enclosure created by the cylinder.

4.1.1 Bearings

To allow for rotation of the cylinders around the central shaft, two slim ball bearings will be placed between each cylinders' inner face and the shaft. These bearings must be lightweight and have very large diameters relative to their height. Kaydon manufactures bearings up to an outside diameter of one meter which meet all of the technical requirements of the MAFSA mission. In order to estimate the mass of a larger bearing, we ran a linear regression on data from the Kaydon NG-series bearings [2] seen in Figure 4. A bearing with an outside diameter of 4 m has a predicted mass of $53.7^{+0.5}_{-0.4}$ kg.

These bearings will be subject to, over a full 10-year mission, approximately 220 full rotations or 110 hours of operation. Typical bearings like these are rated for thousands of hours of continuous operation under full loads making the MAFSA use requirement easily obtainable.

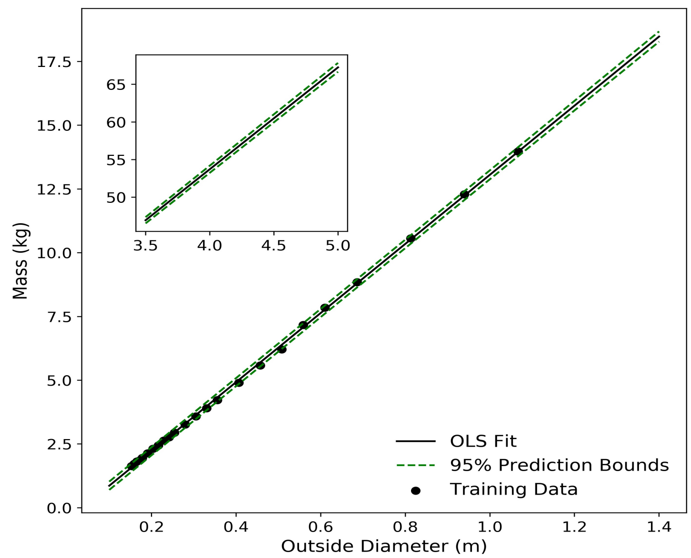

Figure 4: Linear regression of bearing mass on outside diameter

4.1.2 Gears

Rotation of the lower and upper cylinder will be powered by two 250 Nm electric motors stowed inside the hollowed out lower cylinder. A single gear mechanically connects the motor shaft and a gear lining along the inner cylinder wall, as shown in Figure 5. A second gear lining is placed along the top of the lower cylinder that is used to relay the rotational motion to the upper cylinder. As seen in Figure 5, a small hole is cut out of the fixed middle plate so that two gears, fixed to the central shaft, can reach down to the lower cylinder lining and relay rotation to the upper cylinder gear lining. The gear ratio between the upper and lower cylinders is 1.225 to allow for the array and boom to wrap at equivalent rates.

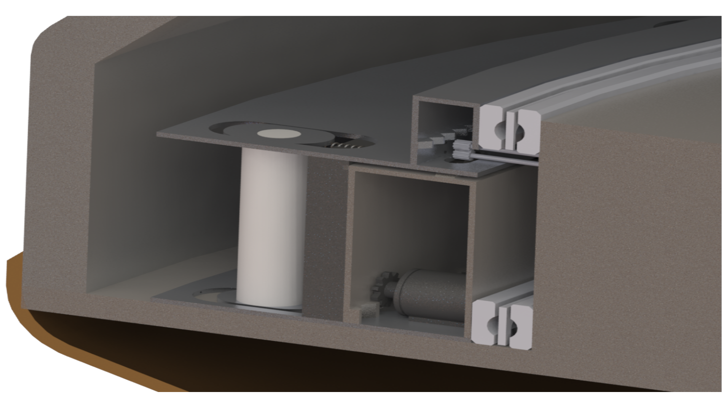

Figure 5: Rotational gear system showing lower and upper cylinder with fixed separating plate. The central shaft has been excluded for visual purposes.

4.2 Booms

A single TRAC boom is 23 m long, including stowed and deployed length, and made from Hexcel® IM7/977-2 carbon fiber composite with a mass density of 1780 kg/m^3. The total mass of the five booms is 626 kg. A boom takes on two different shapes for stowage and deployment.

In the stowed state both flanges are compressed flat together to minimize bending stiffness about the y-axis. This allows the booms to be wrapped around a 360° curvature as long as the radius of curvature is larger than a minimum bound set to prevent fiber failure during stowage.[6]

In the deployed configuration, shown in Figure 6, both flanges are opened to an angle, θ, which allows for a higher bending stiffness about both the x and y axis. Using equations developed by Roccor for these boom geometries [5],[6], MATLAB's *fmincon* optimization function was used given mass, stowed height, strain while wrapped, and twist constraints to find max stiffness. Bending stiffness in the x and y directions are characterized by Equations 1 and 2.

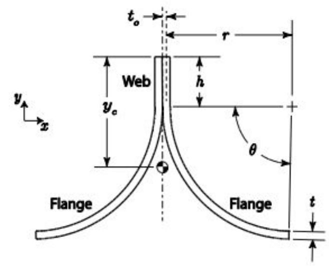

Figure 6: Head on view of TRAC boom [5]

$$I_x = t\frac{h^4 + 12h^2r^2 + 4h^3r\theta + 6hr^3\theta + 6r^4(\theta^2 - 3) - 12r^2cos(\theta)(h^2 - 2r^2) - 6r^4cos(2\theta) - 3r^3sin(2\theta)(h + r\theta)}{6(h + r\theta)} \tag{1}$$

$$I_{y,nom} = \frac{2ht^3}{3} + \frac{rt}{2}(\theta(6r^2 + 4rt + t^2) + 2rsin(\theta)(rcos(\theta) - 2(2r + t))) \tag{2}$$

Where the dimensions are summarized in Figure 6. The mass was constrained to a max of 630 kg and the stowed height was constrained to a max of 35 cm by the volume requirements for the system. Strain while wrapped was constrained to 1.5% determined by the ultimate elongation at failure for IM7 carbon fiber of 1.9%. Strain was determined with Equation 3.

$$\epsilon = \frac{\Delta\kappa t}{2} \tag{3}$$

Where $\Delta\kappa$ is the radius of curvature in the x or y direction and t is the thickness of the boom. Maximum twist due to torque on the boom from the array was set to 10°. Twist of the boom was determined with Equation 4.

$$\phi = \int \frac{T}{GJ} \tag{4}$$

Where T is the torque from array loading (Section 5.3), G is the modulus of rigidity set to 5 GPa, and J is the torsional constant defined for the boom by Equation 5.

$$J = \frac{1}{3}(2(r\theta + h))t^3 \tag{5}$$

Where θ, r, h, and t are defined in Figure 6. The result of the optimization routine was boom dimensions of h=14 mm, r=28 cm, θ=0.63, and t=8.0 mm.

The relationship between two of the four boom dimensions and the bending stiffness is illustrated in Figures 7 and 8. It is important to note that the equations given above are assuming the orientation shown in Figure 6. Orienting the booms with the free end of the flanges facing upwards, where they would be in tension when supporting the solar array, increases the bending stiffness about the x-axis by 3 times compared to a face down orientation [6]. MAFSA utilizes the flange upward approach, opposite to the orientation shown in Figure 6.

Booms are long enough to be wrapped around the circumference of the lower cylinder within the lander module 1.5 times. When fully deployed, each boom will have 2 m of remaining length attached around the cylinder using bolts and braces drilled through the boom and the metal cylinder.

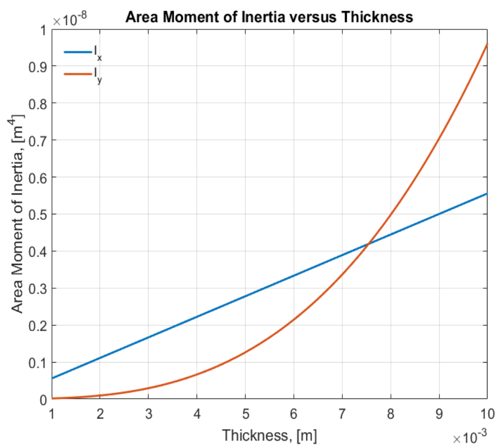

Figure 7: Moment versus boom thickness, t_0

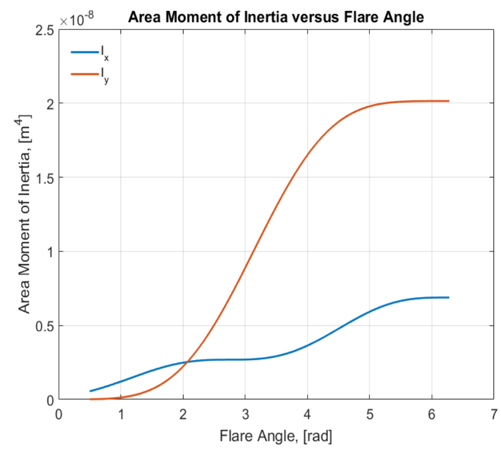

Figure 8: Moment versus flange angle, θ

4.3 Solar Array

The solar array is a single unit that forms a pentagon of 1060 m^2 when deployed with a 20 m^2 circular lander in the center. Each triangular fifth of the array will have 80 evenly spaced segments extending radially from the hub to the end of the triangle. There are two types of guiding lines that form a segment: one is simply an indented path along the array substrate, and the other is formed by a pattern of connection points and openings along a guiding path. The latter allows for open spaces in the array that will be used for dust removal.

The outer edge of the array will be attached to a carbon fiber grating that provides tension along the edge and supports uniform folding and unfolding. The spaced guiding lines are attached to the troughs of the grating, as shown in Figure 9.

The array will rest on top of the booms with the corners of the pentagon attached to the boom ends. A second attachment point will connect the array to the central hub. The point of contact at the hub will be secured using bolts through holes in Kapton that have been reinforced with metal rings. Solar array folds will allow the array to be stowed in a zig-zagging fashion while simultaneously wrapping about the upper cylinder. Each array corner will be attached to the boom ends using a steel cable that wraps around a small stepper motor fixed to the boom, seen in Figure 9. The stepper motor has a thin power cable running through the boom back to the lower cylinder where a controller is connected. When stowed, the motor allows the connecting cable to become slack, allowing compartmentalization of the array and booms. As the booms deploy, the motor begins winding the cable taut to gradually pull the array tight to the booms.

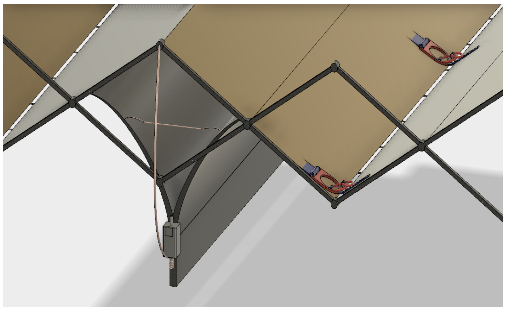

Figure 9: Array grating and attachment to boom

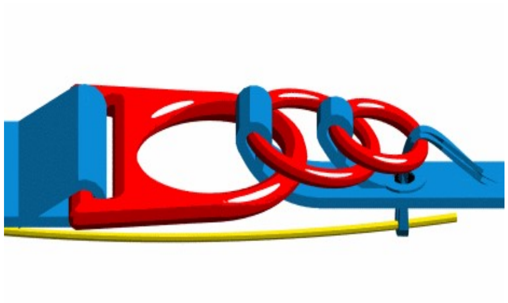

Figure 10: 3-ring system on a skydiving rig [7]

Each segment of the array contains 928 solar cells. A segment will be divided into 20 series strings of 46 cells each to provide 115 V at EOL and accounting for the cell's temperature coefficient. Each string provides a current of 0.47 A at the maximum power point, meaning 20 strings tied in parallel will generate 9.4 A. A 14 gauge wire will form the 115 V bus that each string is tied to. This wire will run through a plastic sheath into the upper cylinder to prevent dust from entering the hub.

To allow for access to the lander while the array is deployed, a series of 3-ring separation mechanisms is used at a pre-existing juncture point along each diagonal of the pentagon array. This 3-ring mechanism is used by skydivers to provide a strong connection of their parachute to the rest of the system and allows for easy separation by pulling a plastic cut-off cord. An example of a 3-ring system can be seen in Figure 10.

If astronauts need to access the lander while MAFSA is deployed, they simply pull the plastic cut-off cord releasing the first set of rings, and continue this process along the length of the array until they reach the lander. To re-attach the array, the astronauts couple the rings back together and re-insert the cutoff cords. This is a simple and proven separation mechanism used millions of times by skydivers.

The mass and volume properties of the MAFSA components described thus far are detailed below in Table 1. MAFSA has a 36.8kg margin below the allocated 1500kg set by NASA and falls well below the volume requirement.

Component	Mass (kg)	Volume (m^3)
Solar Array	508	0.23
Array Grating	22.1	0.012
Booms	626	0.352
Hub	134	0.05
Hub Motors	63.5	0.042
Stepper Motors	4	0.0002
Bearings	110	0.287
Total	1463.2	1.73
Allocated Total	1500	10.0
Margin	32.4	8.31

Table 1: Summary of mass and volume for each primary component. The total volume of the components provided does not include space within the module. The stowage design took advantage of the total 10 m^3, leaving 9.4 m^3 of space within the module, and providing flexibility to design changes or added functions, such as energy storage.

4.4 Lander Integration

At this stage in the design, MAFSA does not require a particular geometry or configuration of the lander. The MAFSA module is cylindrical, but because it integrates with the lander via a central shaft, the shape of the lander above and/or below does not need to match the MAFSA module. Other than the central shaft, the components in the module are not directly connected nor provide support to the lander.

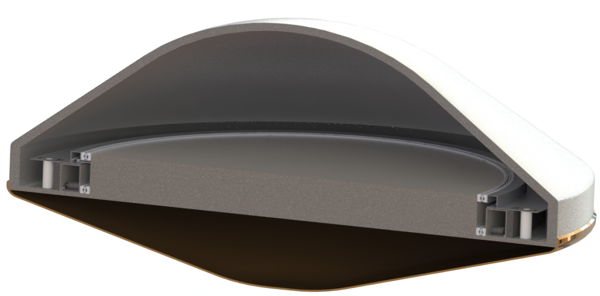

Figure 11: MAFSA shown as a modular stowage load in a conceptual Martian lander capsule

The MAFSA module can be positioned at various vertical levels within the lander. The minimum height above the Martian surface is constrained by the max deflection to prevent dragging of the booms or hitting large obstacles during deployment and retraction. From Figure 12 the max downward deflection is 25 cm. To prevent hitting obstacles over 50 cm, the minimum height of the module from the Martian surface should be 75 cm. The module can then be positioned within the lander at any height above this minimum.

Upon landing on the Martian surface the sides of the landing module will eject and expose the MAFSA module. The general integration of MAFSA with the lander is shown in Figure 11.

5 Mission Plan

5.1 Module Assembly

The MAFSA module can be assembled starting from the center and building radially outward. The central shaft is the core of the module and connects the module to the lander. Bearings are then placed between the central shaft and the rotating cylinders for the booms and the array. The hollowed rotating cylinders are next, with the motors and gears within. The booms and array are attached to the outside of the cylinders. Lastly, the guiding rollers and supports are placed around the booms between the base plate and mid plate. A cross section of the MAFSA module can be seen in Figure 5.

5.2 Deployment and Retraction

Deployment of MAFSA's booms and array takes approximately 30 minutes. Assuming the motor being used is operating at maximum torque of 270 Nm over the course of constant rotational speed, the total amount of energy required by the motor for deployment is 0.69 kWh. Retraction is accomplished by simply reversing the motor direction.

Initial designs called for supporting legs at the end of each boom. After further analysis, it was determined that only support at the central hub in the deployed state is necessary. Figure 12 shows deflection of the booms and confirms that legs are not required for support outside of the central hub. Eliminating supporting legs greatly reduces frictional forces while deploying and retracting, minimizing the risk of buckling and permitting predictable mechanical behavior. The problems that large obstacles pose to full deployment is also mitigated by eliminating legs.

Forces that could adversely affect smooth deployment and retraction still exist. Most notably, friction between the boom and the lower plate of the hub and pressure from the brush sweeping dust during retraction. The former is minimized by placing rollers under the booms on the base plate. The rollers reduce the maximum torque needed to deploy the booms to under 10 Nm, assuming friction-less bearings, while the motors can each produce a torque up to 270 Nm. If the rollers fail, the peak coefficient of friction between aluminum and carbon fiber is 0.68 [8], giving a max torque of 285 Nm which can still be overcome with both motors if necessary. Dust in the booms is minimized through periodic partial and full retractions which prevent significant dust accumulation in the booms. The rate of dust accumulation in the booms is low (on the order of $1\text{x}10^{-5}$ kg/sol, see Section 5.4.1) and as a result the additional force exerted to sweep dust is overcome by the motor.

After the initial deployment, subsequent retractions and deployments are driven by dust and storm mitigation discussed in detail in Sections 5.4.2 and 5.4.3. It is important to also minimize the amount of retractions per year to increase the lifetime of the mechanical components and to mitigate the risks associated with retraction. MAFSA will be programmed to partially retract an average of 17 times per year for dust removal, with full retractions occurring, on average, once or twice a year during severe dust storms. The operating time for the mechanical components as a result of retraction and deployment is around 11 hours per year. This operating time is minimal for the parts chosen so long as dust is prevented from entering the bearings, gears, and motor area.

5.3 Deployed State

In the deployed state the array rests on top of the five booms, connected only to the boom ends and the central hub. Two simulations were performed to investigate the loading on the booms from the array in the deployed state. The results confirm that the booms could support the array to a first order approximation.

The first simulation quantified the downward deflection along the length of the boom. Based on the results from Roccor, the moment of inertia for the v-up orientation used here is 3 times greater than the moment of inertia for the orientation given in Figure 6. The array was modeled as a flat, uniform load for simplification. This is a reasonable approximation due to the small angles off the horizontal ($\approx 5°$) in the deployed state and the constant density throughout the array. Figure 12 shows the result of the simulation.

A max deflection of 25 cm occurred at the end of the boom. The bending stress of the boom was 67 MPa, well under the estimated max flexural strength of 1,800 MPa for an IM7 carbon fiber composite. Based on this result, it was decided that legs to support the booms at the perimeter would not be necessary.

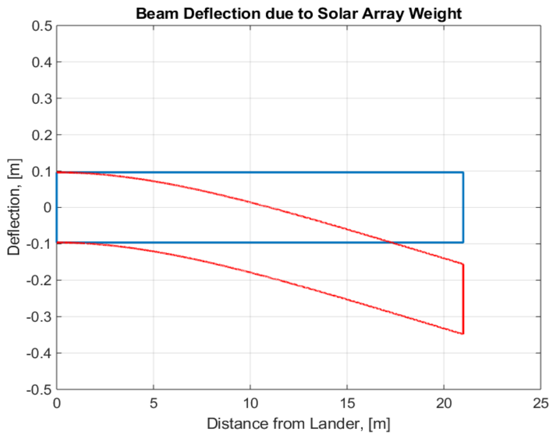

Figure 12: Boom deflection under weight of solar array

Finite element method (FEM) was used to quantify the moments along the boom due to non-symmetric loading. Torque is crucial to quantify because the booms have a lower torsional stiffness and enough torsion will cause the booms to fail. In the simulation, the array was assumed to be flat and connected to the boom outer edge along the boom length. The results of the FEM are shown in Figure 13. The maximum reaction torque along the boom is ≈6 Nm. Figure 14 shows the boom's twist angle as a result of the reaction torque using Equation 4 and assuming the maximum twist angle to be 10°. At this time, it is thought that the boom will not fail with a max torsion of 10°. However, further characterization of the boom and the torque it can withstand given the MAFSA dimensions is necessary.

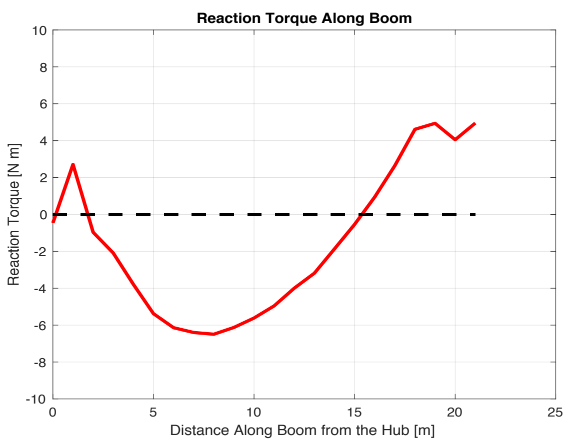

Figure 13: Torque on boom from FEM analysis

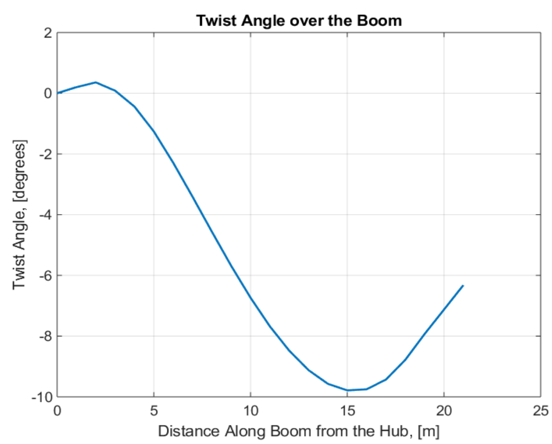

Figure 14: Torsion along the length of the boom

5.4 Operation

During operation MAFSA must meet 3 primary requirements over a 10 year time span and within a highly variable Martian surface environment. The requirements are power generation, dust removal, and storm mitigation.

5.4.1 Dust Accumulation

The rate of dust settling on the array is important to quantify to both ensure the array structure will not overload the booms and to maximize efficiency of power generation. It has been estimated using gravitational settling with Stoke's Law that dust settles on the Martian surface at a rate of 30,000 particles/cm^2/sol on average [9]. This rate can increase to 240,000 particles/cm^2/sol during storms and decrease to as low as 1,200 particles/cm^2/sol. To estimate the mass increase associated with these settling rates one also needs to know the size and density of the dust. The geometric mean radius of dust particles is estimated to be 1.85 ± 0.3 m from analysis of Viking Lander images [10]. Lastly, bulk density of the dust is estimated to be 1,520 kg/m^3 obtained from analysis of Pathfinder data [11]. Using these estimates and sampling from a normal distribution of particle sizes, the mean rate of mass increase on the array is 0.01 kg/sol with a worst case scenario of 0.1 kg/sol during storms. These rates indicate that mass overloading of the booms is not a significant concern and removing mass will not be the primary driver for retraction of the array.

In contrast to mass loading, dust accumulation on the arrays does have a significant impact on power generation efficiency. Analysis of Pathfinder data found a daily efficiency loss (obscuration) of 0.28% [12]. A simulation was run over 100 years to quantify the long-term trends of the obscuration rate by sampling from a gamma distribution with a mean of 0.28%. Sampling from a gamma distribution ensures that most days are average or less than average in obscuration percentage while still allowing for rare but large dust storms. The simulation was set up to initiate dust removal after an obscuration of 5%, returning the obscuration to a low normal random variable (accounting for imperfect dust removal). Figure 15 shows the outcome of the simulation. It is evident that obscuration can be well above 5% during days of heavy dust deposition (up to 12% obscuration) but on average the max obscuration will be roughly 5% which means the array will produce within 95% of its maximum efficiency over its lifetime.

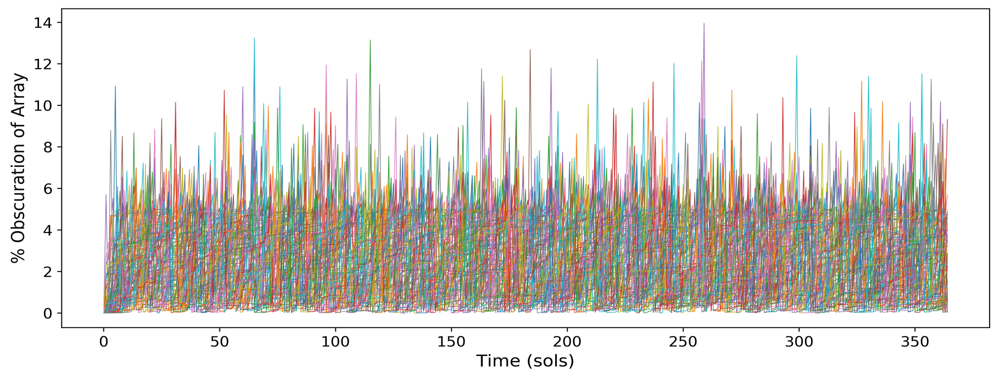

Figure 15: Simulation over 100 years for dust obscuration assuming cleaning events when obscuration is above 5%. Each color represents an indivdual year.

The results of this 100 year simulation were used to estimate the amount of mitigation events that happen in an average year assuming a maximum obscuration percentage of 5%. Figure 16 below shows an example of the low (top), average (middle), and max (bottom) mitigation events in a year sampled from the 100 years simulation. The average number of mitigation events in a year is 17 setting the MAFSA system to conduct dust mitigation every 21 days. The obscuration may be more or less than 5% at each cleaning but establishing an automatic retraction schedule is simple to implement and produces a reasonable balance between minimizing retractions over time and maximizing power production.

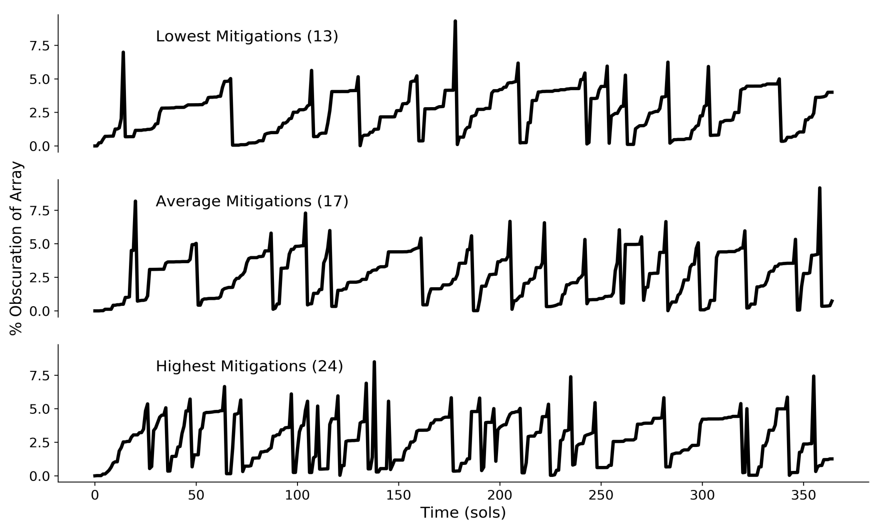

Figure 16: Example years from the 100 years simulation for the lowest (top), average (middle) and highest (bottom) number of mitigation events.

5.4.2 Power Generation

MAFSA is capable of generating 15 kW to 30 kW of equivalent continuous power over a Martian year at the equator. This was calculated using the annual global irradiance profile given by NASA, the solar cell efficiency at end of life, modeling of dust coverage and mitigation, and an ideal daily irradiance profile. Power generation estimates considered the array to be flat. This is a reasonable approximation because the array will be between 5-10° from the horizontal. An angle of 5-10° corresponds to a minimal decrease in efficiency (98-99%) compared to a flat array case when the Sun is directly overhead. At lower Sun angles the power production matches the flat case over the course of a sol due to symmetry in the array shape and folding.

The daily power output shown in Figure 17 is for a dustless 9 hour day at maximum annual irradiance. Due to the expanse of the array compared to the lander profile, the lander shadow does not produce significant variation in the daily power generation of the solar array. An annual daily continuous power output, shown in Figure 18, was developed using the average power output over a single day as the continuous power equivalent, and assuming 21 sol cleaning events restore the array to 98% efficiency. There is a total energy loss over the course of a Martian year of only 5% from the case without dust obscuration.

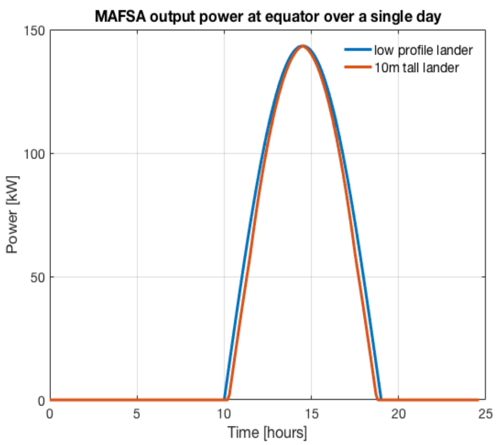

Figure 17: Daily power output with ideal solar profile accounting for lander shadow.

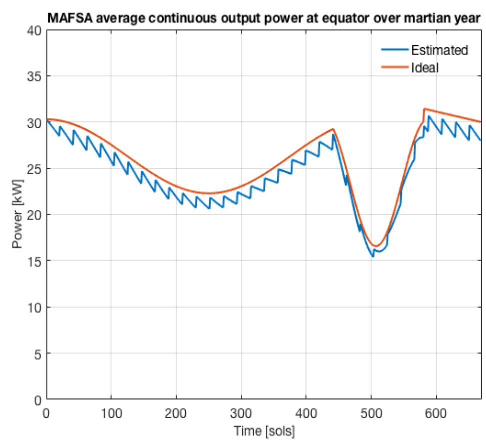

Figure 18: Annual equivalent continuous power output with dust storm event shown at ≈450 sols.

5.4.3 Dust Removal and Mitigation

Dust and debris removal are a necessary consideration for a solar array to operate efficiently and autonomously on the surface of Mars for 10 years. The folded design of MAFSA provides a straight-forward mechanism to prevent dust build up on the photovoltaic surface. In the stowed state, the angle between folds will be effectively 0°, while in the fully deployed state, the angle between folds will be approximately 170°. Thus, even in the deployed state, the panel is never perfectly flat, and is instead a series of peaks and troughs. As dust settles into the troughs, it falls through slits in the substrate and back to the ground. However, a 170° angle between each fold in the deployed state means each fold is 5° from horizontal. The angle needed to overcome the frictional force can be found by the simple relationship μ_f=tan(θ), where μ_f is the coefficient of friction between the dust and photovoltaic material and θ is the angle of the solar array fold from the horizontal. Most dry materials have a coefficient of friction between 0.3 and 0.6, which means the array fold must have an angle between 17° and 31° from the horizontal.

Van der Waals adhesion force is more difficult to quantify but is significant at the micrometer dust particle size scales [13]. The adhesion force can be overcome with the same method used to overcome frictional forces. However, this requires a steeper angle of 45° from the horizontal found from laboratory experiments with Mars dust simulants [14]. Retraction to 45° happens at night, and allows time for dust to fall or be blown off by natural winds. The array would retract by 11 m to reach the desired angle, consuming 0.3 Wh, a relatively small energy cost.

In summary, dust removal from the array will be accomplished by retracting the array to an angle of 45° once per 21 nights (determined in Section 5.4.3) and then returning to the fully deployed state before sunrise. This mechanism provides a simple but effective dust mitigation strategy with low energy costs that fits naturally with the structural design of the array. It does not rely on mechanical vibration or forms of an electromagnetic dust shield which add significant complexity and are unproven for structures of this size.

Dust can also accumulate in the inner volume of the booms. The rate of accumulation will be minimal but over 10 years of operation or after a severe dust storm the dust inside the boom could produce significant loading. A V-shaped brush positioned just outside the central hub will sweep dust out of the array during retraction. Inevitably, dust will pass the brush and begin to accumulate at the interior of the brush during re-deployment. There will be small holes near the web of the boom just inside the brush at full extension. Once the system begins to extend, the brush will serve as a second barrier and any remaining dust caught on the hub side will fall into the holes back to the Martian surface after re-deployment.

Lastly, dust mitigation within the central hub is crucial for successful operation over the array's lifetime. The central hub is designed so the only parts exposed to the Martian environment are the booms, the array, and the outer cylinder which the booms and array wrap around. The motor, bearings, and gears are all within the outer cylinder (see Figure 5) protected from the Martian environment. Plastic trim and rubber rings (permitting a rubber material can be found to withstand the extreme temperature variation) will be used at the base of the upper and lower cylinders to prevent dust from entering the gaps between the fixed and rotating components.

5.4.4 Storm Mitigation

Dust storms on Mars can last for months and produce winds up to 50 m/s. While the atmosphere has a density of only 0.02 kg/m^3 at the surface ($\approx$ 60x less than Earth's atmospheric surface density), storms could still have detrimental effects, given the area of the deployed array, it's low-mass, and size of the supporting booms. In the case of intense storm events, the array can be retracted and stowed as described in Section 5.2. However, the array cannot be in a stowed state for every storm event because power will be needed continuously for human and ISRU operations.

A series of simulations were performed to understand the effects of a storm on the deployed array. To simplify the aerodynamic analysis, it was assumed that the boom could be modelled as a flat plate perpendicular to the flow. Under this assumption, the coefficient of drag is 1.28 [15]. The deflection was calculated assuming a uniform load given by the drag per unit length. Figure 19 shows the deflection in the boom due to aerodynamic forces in a 50 m/s flow. The boom is being viewed from above, the lander is to the left, and the uniform flow is coming from the bottom of the plot. The max bending stress on the boom for 50 m/s wind is 119 MPa which is well under the estimated max flexural strength of 1,800 MPa for an IM7 carbon fiber composite.

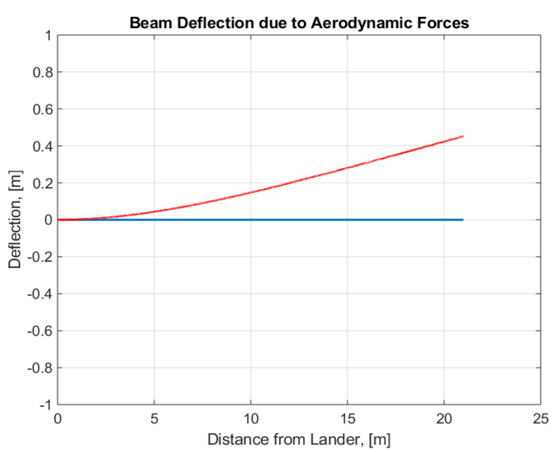

Figure 19: Boom deflection with 50 m/s winds

The size of MAFSA's flexible surface area raises an additional concern from the aero-elastic effects of storms. However, due to the complex interaction between the structure and the turbulent aerodynamics around MAFSA, a detailed, formal analysis is beyond the scope of this work. Steps have been taken to mitigate the risk of failure. Specifically, the flexible solar array's movement is constrained on the outer boundary, air is allowed to escape from underneath through the holes that are also used for dust mitigation, and the array will be retracted during storms with high winds.

6 Risk Analysis

Using the latest version of the NASA S3001 ”Guidelines for Risk Management”[16] document, the risks associated with the MAFSA mission are detailed below.

1. **Single Motor Failure (while deployed/partially deployed)**

   In the case of a single motor failure, MAFSA can continue standard operations with the second motor which individually supplies the power needed for deployment and retraction. However, the system is at heightened risk of complete failure due to dependency on a single motor, especially considering the added work on the motor.

   To mitigate this failure mode, the driving motor should be carefully selected and modified to minimize the amount of Martian dust that enters the motor windings. The central hub has been designed to isolate the motors from the outside environment as described in Section 5.4.3.

2. **Total Motor Failure**

   In the case of both motors failing after full deployment or during deployment/retraction, multiple scenarios exist. If fully deployed, MAFSA will still be capable of power generation but will lose the ability to mitigate dust build up on the array. If the motors were to fail while partially deployed, the effect on power generation would roughly depend on how extended the array is and thus each panels angle off nadir.

   If the driving motors were to fail while MAFSA was completely retracted, the mission would end, and power generation would cease. This is the most extreme failure mode for the MAFSA mission, but would only occur due to retracting during storm time events. As such, this failure mode has a very low probability of occurring.

   The mitigation for total motor failure is the same as in the single motor case with the addition that two motors were used to minimize this risk.

3. **Impact of boom with Martian debris**

   During deployment, it is possible that the end of a boom will contact a large obstruction. If the boom encountered an obstruction and quickly cleared itself via the force from the driving motor causing the boom to sheer off to one side, then there would likely be no immediate impact to the mission. If however, the boom encountered an obstruction and did not automatically clear itself, then the boom may break due to the force of the driving motor. This failure would lead to part of the array deploying in an anomalous fashion and keep the array from retracting for the remainder of the mission. Power generation would depend upon the integrity of the circuitry along the boom and the new geometry of the effective photovoltaic area in relation to the Sun.

   The most robust way to prevent these failures is to pick a landing sight which does not contain obstructions up to the height of the deploying booms. It is assumed by MAFSA that the landing zone would be highly constrained, and landing vehicles would be able to hit their mark with a high degree of accuracy. The MAFSA module is adaptable and can be placed at a higher positions in the lander to pass over smaller obstacles. In the case of an uncertain landing area which may contain large obstructions, the MAFSA system may employ a LiDAR or similar system to map its surroundings before deploying. The system would need to identify objects in the path of the extending booms and give the system a maximum length to deploy the array.

4. **Dust build up on the solar array**

   While deployed on the Martian surface, the solar array will gradually become covered in dust reducing the systems ability to generate power nominally. The MAFSA system addresses dust build up on the solar arrays by periodically retracting the array just until the angle off nadir is sufficient that gravity pulls the dust off the array and through holes between individual panel sections.

5. **Dust intrusion into mechanical parts**

   Over time, it is possible that dust may enter mechanical parts and hinder their ability to function nominally. MAFSA employs a variety of mitigation strategies organized by major part below.

(a) Booms

The MAFSA booms are a V shape which over time could fill with Martian dust. The weight of this dust would eventually cause the booms to fail structurally and thus must be cleared periodically. The MAFSA system will use a brush attached to the hub which extends into the V-shape of the boom described in Section 5.4.3.

(a) Motor

See risks one and two above

(a) Bearings

To allow for the rotation of the central hub, MAFSA employs two sets of ball bearings which sit between the central core and the upper or lower structure of the hub. These ball bearings are particularly important to shield from dust intrusion since their nominal function allows for deployment and retraction of the system. MAFSA employs plastic trimming and plastic microfibers to seal the gap between the mid-plate and the boom hub so that dust is not allowed to enter the gears, motor, and bearing enclosure.

6. **Martian storms**

There will be multiple storms during the MAFSA mission which could generate destructive forces on the solar array if deployed. These storms happen several times a year and thus must be dealt with in the operations design of the system. The MAFSA system will avoid storms almost entirely by completely retracting the array until winds calm down to sustained safe levels. The array and mechanical parts are still subject to increased dust intrusion but this effect is minimal due to the dust mitigation strategies employed by MAFSA.

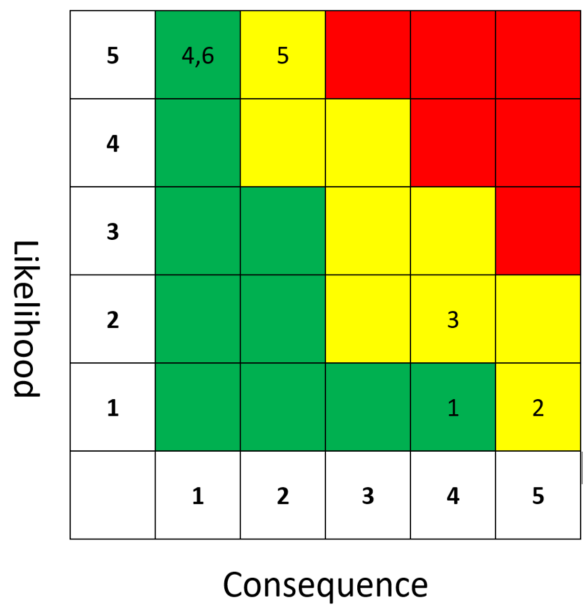

Figure 20: Risk matrix for the failure modes described above

7 Future Work

First order analysis of MAFSA to this point demonstrates the potential of the design to successfully operate on Mars. However, more robust analyses and experiments are necessary to characterize the booms and solar array and prove the overall structural integrity and reliability of the mechanical functions.

The most important work is detailed characterization of structural performance of the scaled-up TRAC booms and generating comprehensive FEM models. The TRAC boom designs are known to have lower torsional stiffness than bending, and torsional stiffness can lead to the boom buckling [5]. The expected torsional load is primarily due to the asymmetrical loading by the solar array. Minimizing torque on the booms over the mission lifetime will therefore be a primary driver in optimizing both the boom and hub design. This can be accomplished by optimizing the folding patterns and adding intentional weight imbalances in the array so that the asymmetrical geometry between boom and array produces a symmetrical weight distribution.

Additionally, the structure's response to loading needs to be investigated further. Here, the analysis has been performed with linear analysis. Roccor, however, has reported that at high deflections the booms act non-linearly. In [5] and [6], Roccor used non-linear FEA to model the booms. Although the small deflection of about 1% of the total length of the booms is expected to be within the linear region, a similar analysis will need to be conducted here. The nonlinear FEA also should be used to consider the coupled behavior of the structure. Due to the open cross section of the TRAC booms, any lateral load is expected to induce a torsional load on the boom.

Finally, to simplify the design of the boom presented here, it has been based on the results from Roccor which uses IM7/977-2 carbon fiber composite. Further analysis should be done into the design of the laminate. For example, M55J carbon fiber may be used to improve the bending stiffness of the material, however the increased stiffness may cause issues with wrapping. Additionally, the orientation of the plies may change the behavior of the composite.

In the case of the array, we have assumed that upon retraction the array will compact to its stowed shape. Deployable arrays in space are not typically designed to retract and as a result the total flight readiness is low for folding patterns and mechanisms to produce repeated, predictable deployed and stowed states. The MAFSA folding pattern, grating, and mechanical design will need to be tested and refined for ideal performance.

8 Conclusion

The Mars Autonomous and Foldable Solar Array is a solution for the power production demands to support human activity on Mars. MAFSA is a low mass, mechanically simple design, with the structural stability to withstand the dynamic Martian surface. The design expands upon technologies that are currently in development, most notably, the Roccor TRAC booms, but also, includes novel ideas (i.e. solar array stowage and deployment folding and dust mitigation strategies) necessary to meet the large solar surface area requirements and power performance. The folded nature of the array substrate is a crucial aspect of the design that provides structural rigidity in the deployed state, allows for guided, predictable deployment and retraction, and provides a natural dust mitigation mechanism. MAFSA is a self-contained unit that can be integrated on a variety of lander platforms, and meets the set-forth requirements for a solar array to support humans on Mars.

Acknowledgements

We would like to first thank Kamron Medina from Roccor for his help in determining TRAC boom characteristics through shared papers, tours of their facility, and availability for technical questions. We would also like to thank Professor Francisco Jimenez for sharing his knowledge in deployable space structures and mechanical analysis. Finally, we would like to thank Yasara Dharmadasa for running Abaqus FEA for various configurations of our deployed geometry.

References

[1] C. Pearson. Roccor TRAC boom data sheet. 2017.

[2] Kaydon. Kaydon Bearing Solutions. https://www.kaydonbearings.com/Endurakote_bearings_NG_typeC.htm.

[3] D.C. Law et al. Lightweight, flexible, high-efficiency, III-V multijunction cells. *Area 6: Poster Session I-Space Cells and Radiation effects*.

[4] J. Carr et al. Lightweight integrated solar array and transceiver. *Small Satellite Conference*, 2016.

[5] T.W. Murphey L.G. Adams, D.E. Turse. TRAC boom structural mechanics. *American Insititute of Aeronautics and Astronautics*.

[6] J.A. Banik T.W. Murphey. Performance validation of the triangular rollable and collapsible mast. *24th Annual AIAA/USU Conference on Small Satellites*.

[7] Denis Yusupov. 3-ring animation, 2011. https://commons.wikimedia.org/wiki/File:3Ring_release_animation.gif.

[8] Joakim Schn. Coefficient of friction for aluminum in contact with a carbon fiber epoxy composite. *Tribology International*, 37(5):395 – 404, 2004.

[9] G.A. Landis. Dust obscuration of Mars photovoltaic arrays. *Acta Astronautica*, 38.

[10] James Pollack et al. Viking Lander image analysis of martian atmopheric dust. *Journal of Geophysical Research*, 100.

[11] S.F. Hviid et al. Magnetic properties experiments on the Mars Pathfinder Lander: Preliminary results. *Science*, 278.

[12] T.W. Kerslake L.L. Kohout. Solar electric power system analysis for mars surface missions. *34th Intersociety Energy Conversion Engineering Conference*, July 1999.

[13] G.A. Landis P.P. Jenkins. Dust mitigation for Mars solar arrays. *IEEE*, May 2002.

[14] James Gaier Mark Marabito, Marla Perez-Davis. Aeolian removal of dust types from photovoltaic surfaces on Mars. *16th Space Simulation Conference*, November 1990.

[15] NASA Glenn Research Center. Shape effects on drag, 2015. https://www.grc.nasa.gov/WWW/k-12/airplane/shaped.html.

[16] NASA. S3001: Guidelines for risk management. 2017.